

# Non-Abelian topological phases in an extended Hubbard model

Michael Freedman,<sup>1</sup> Chetan Nayak,<sup>1,2</sup> and Kirill Shtengel<sup>1</sup>

<sup>1</sup>Microsoft Research, One Microsoft Way, Redmond, WA 98052

<sup>2</sup>Department of Physics and Astronomy, University of California, Los Angeles, CA 90095-1547

(Dated: November 2, 2018)

We describe four closely related Hubbard-like models (models *A, B, C* and *D*) of particles that can hop on a 2D Kagomé lattice interacting via Coulomb repulsion. The particles can be either bosons (models *A* and *B*) or (spinless) fermions (models *C* and *D*). Models *A* and *C* also include a ring exchange term. In all four cases we solve equations in the model parameters to arrive at an exactly soluble point whose ground state manifold is the extensively degenerate “*d*-isotopy space”  $\bar{V}_d$ ,  $0 < d < 2$ . Near the “special” values,  $d = 2 \cos \pi/k + 2$ ,  $\bar{V}_d$  should collapse to a stable topological phase with anyonic excitations closely related to SU(2) Chern-Simons theory at level *k*. We mention simplified models *A*<sup>-</sup> and *C*<sup>-</sup> which may also lead to these topological phases.

## I. INTRODUCTION

Since the discovery of the fractional quantum Hall effect in 1982<sup>1</sup>, topological phases of electrons have been a subject of great interest. Many abelian topological phases have been discovered in the context of the quantum Hall regime<sup>2</sup>. More recently, high-temperature superconductivity<sup>3,4,5,6,7,8,9,10,11,12,13,14,15,16</sup> and other complex materials have provided the impetus for further theoretical studies of and experimental searches for abelian topological phases. The types of microscopic models admitting such phases is now better understood<sup>17,18,19,20</sup>.

Much less is known about non-abelian topological phases. They are reputed to be obscure and complicated, and there has been little experimental motivation to consider non-abelian topological phases, apart from some tantalizing hints that the quantum Hall plateau observed at  $\nu = 5/2$  might be non-abelian<sup>21,22,23,24,25,26,27</sup>. However, non-abelian topological states would be an attractive milieu for quantum computation<sup>28,29</sup>. Furthermore, a better understanding of non-abelian topological phases would help determine if they have already been unwittingly observed in nature. It is, therefore, encouraging that recent progress in understanding the Hamiltonian formulation of a class of topological field theories has reduced computations in these theories to combinatorial-pictorial manipulations<sup>30,31</sup>. These theories do not break parity or time-reversal symmetry, which may have practical advantages. A further virtue of this formulation of these theories is that it exposes a strategy for constructing microscopic physical models which admit the corresponding phases; since Hilbert space is reduced to a set of pictorial rules, the models should impose these rules as energetically-favorable conditions satisfied by the ground state. In this paper, we show how this approach can be implemented.

The microscopic models which we construct are ‘quasi-realistic’. Their precise form is not likely to be realized in any material. However, they are soluble, so we know that they do, indeed, support the non-abelian topological states of matter which interest us, and one can imagine a real material whose Hamiltonian can be viewed as a small perturbation of one of the Hamiltonians of this paper. It may also be possible to design a quantum dot or Josephson junction array with such a Hamiltonian.

The non-abelian topological phases which arise in this paper are related to the doubled SU(2)<sub>*k*</sub> Chern-Simons theories described in Refs. 31,32. In appendix A some further information about these theories, called  $\mathcal{DK}_k$ , is given<sup>48</sup>. For the moment, we note that  $\mathcal{DK}_k$  has ground state degeneracy  $(k+1)^2$  on the torus  $T^2$  and should be viewed as a natural family containing the topological (deconfined) phase of  $\mathbb{Z}_2$  gauge theory as its initial element,  $k = 1$ . For  $k \geq 2$  the excitations are non-abelian. For  $k = 3$  and  $k \geq 5$  the excitations are computationally universal<sup>33,34</sup>. In Appendix B some general purpose formulae for the perturbation theory of Hubbard models are derived.

The basic strategy of the present paper is to construct a Hamiltonian which enforces a subset – *d*-isotopy<sup>31,32</sup> – of the defining conditions of the Hilbert space of these theories. The resulting low-energy subspace will be called  $\bar{V}_d$ . It has been argued<sup>31,32</sup> that for special values of the parameter *d*, namely  $d = 2 \cos(\pi/k + 2)$ ,  $\bar{V}_d$  will collapse to the stable topological phase  $\mathcal{DK}_k$ .

## II. THE BASIC MODEL

The models described in this paper, both bosonic and fermionic, are defined on the Kagomé lattice. The basic lattice is shown in Fig. 1. The sites of the lattice are not completely equivalent, in particular we choose two special sublattices –  $\mathcal{R}$  (red) and  $\mathcal{G}$  (green) whose significance shall become clear later on. In some cases we will introduce “defects” in this sublattice arrangement.

Our generic Hamiltonian is given by:

$$H = \sum_i \mu_i n_i + U_0 \sum_i n_i^2 + U \sum_{(i,j) \in \mathcal{O}} n_i n_j + \sum_{(i,j) \in \mathcal{B}, \neq \mathcal{O}} V_{ij} n_i n_j - \sum_{\langle i,j \rangle} t_{ij} (c_i^\dagger c_j + c_j^\dagger c_i) + \text{Ring}. \quad (1)$$

Here  $n_i \equiv c_i^\dagger c_i$  is the occupation number on site *i*,  $\mu_i$  is the corresponding chemical potential.  $U_0$  is the usual onsite Hubbard energy  $U_0$  (clearly superfluous for spinless fermions).  $U$  is a (positive) Coulomb penalty for having two particles on the same hexagon while  $V_{ij}$  represent a penalty for two particles occupying the opposite corners of “bow ties” (in other words,

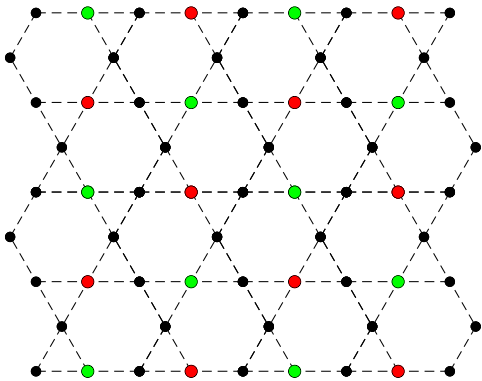


FIG. 1: Kagomé lattice  $\mathcal{K}$  with the special sublattices  $\mathcal{R}$  (depicted red) and  $\mathcal{G}$  (green).

being next-nearest neighbours on one of the straight lines). We allow for the possibility of inhomogeneity so not all  $V_{ij}$  are assumed equal. Specifically, define  $v_{ab}^c = V_{ij}$  where  $a$  is the color of site ( $i$ ),  $b$  is the colour of ( $j$ ), and  $c$  is the colour of the site between them. In the lattice in Fig. 1 we have, possibly distinct,  $v_{bb}^g, v_{bb}^b, v_{bg}^g, v_{rb}^b$ , and  $v_{rg}^g$ , where  $r \in \mathcal{R}$ ,  $g \in \mathcal{G}$ , and  $b \in \mathcal{B} = \mathcal{K} \setminus (\mathcal{R} \cup \mathcal{G})$ .  $t_{ij}$  is the usual nearest-neighbour tunnelling amplitude which is also assumed to depend only on the colour of the environment:  $t_{ij} \equiv t_{ab}^c$  where  $c$  now refers to the colour of the third site in a triangle. Finally, “Ring” is a ring exchange term – an additional kinetic energy term which we add to the Hamiltonian on an *ad hoc* basis to allow correlated multi-particle hops which “shift” particles along some closed paths (see more on this term below). Ring exchange terms can be justified semiclassically, but are not generally included as bare terms in the Hubbard model<sup>49</sup>. In models  $B$  and  $D$  we remove the Ring term at the expense of complicating the sublattice  $\mathcal{R}$  (and thus the interactions) with the addition of several new colors.

The onsite Hubbard energy  $U_0$  is considered to be the biggest energy in the problem, and we shall set it to infinity, thereby restricting our attention to the low-energy manifold with sites either unoccupied or singly-occupied. The rest of the energies satisfy the following relations:  $U \gg t_{ij}, V_{ij}, \mu_i$ ; we shall be more specific about relations between various  $t_{ij}$ ’s,  $V_{ij}$ ’s and  $\mu_i$ ’s later.

We are particularly interested in the 1/6-filled case (i.e.  $N_p \equiv \sum_i n_i = N/6$ , where  $N$  is the number of sites in the lattice). The lowest-energy band then consists of configurations in which there is exactly one particle per hexagon, hence all  $U$ -terms are set to zero. (One example of such a configuration is given by particles occupying all sites of sublattice  $\mathcal{R}$ .) These states are easier to visualise if we consider a triangular lattice  $\mathcal{T}$  whose sites coincide with the centers of hexagons of  $\mathcal{K}$ . ( $\mathcal{K}$  is a *surrounding* lattice for  $\mathcal{T}$ .) Then a particle on  $\mathcal{K}$  is represented by a dimer on  $\mathcal{T}$  connecting the centers of two adjacent hexagons of  $\mathcal{K}$ . The condition of one particle per hexagon translates into the requirement that no dimers share a site. In the 1/6-filled case this low-energy manifold coincides with the set of all dimer coverings (perfect matchings) of  $\mathcal{T}$ . The “red” bonds of  $\mathcal{T}$  (the ones corresponding to the sites of

sublattice  $\mathcal{R}$ ) themselves form one such dimer covering, a so-called “staggered configuration”. This particular covering is special: it contains no “flippable plaquettes”, or rhombi with two opposing sides occupied by dimers (see Fig. 2).

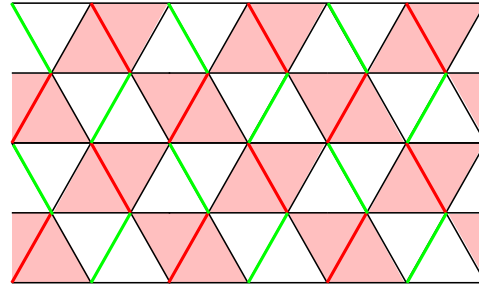


FIG. 2: Triangular lattice  $\mathcal{T}$  obtained from  $\mathcal{K}$  by connecting the centers of adjacent hexagons. The bonds corresponding to the special sublattices  $\mathcal{R}$  and  $\mathcal{G}$  are shown in red and green correspondingly. See text for more on bond color-coding. Triangles with one red side are shaded as guide to the eyes: these triangles will be essential for the dynamics of our models.

So henceforth particles live on *bonds* of the triangular lattice (Fig. 2) and are represented as dimers<sup>50</sup>. In particular, a particle hop corresponds to a dimer “pivoting” by  $60^\circ$  around one of its endpoints,  $V_{ij} = v_{ab}^c$  is now a potential energy of two parallel dimers on two opposite sides of a rhombus (with  $c$  being the color of its short diagonal).

From the relation to dimer coverings exhibited above, it is clear that our model is in the same family as the quantum dimer model<sup>35</sup>, which has recently been shown to have an abelian topological phase on the triangular lattice<sup>17</sup> which, in the notation of this paper, is  $\mathcal{DK}_1$ . Here, we show how other values of  $k$  can be obtained.

The goal now is to derive the effective Hamiltonian acting on this low-energy manifold represented by all possible dimer coverings of  $\mathcal{T}$ . Our analysis is perturbative in  $t/U =: \epsilon$ .

The initial, unperturbed ground state manifold for  $U_0 = \infty$ ,  $U$  large and positive, all  $t_{ij}, V_{ij} = 0$  and all  $\mu_i$  equal is spanned by the dimerizations  $\mathcal{D}$  of the triangular lattice  $\mathcal{T}$ . As we gradually turn on the  $t$ ’s,  $v$ ’s, and Ring terms, we shall see what equations they should satisfy so that the effective Hamiltonian on  $\mathcal{D}$  has the desired space  $\bar{\mathcal{V}}_d$  as its ground state manifold (GSM).

Since a single tunnelling event in  $\mathcal{D}$  always leads to dimer “collisions” (two dimers sharing an endpoint) with energy penalty  $U$ , the lowest order at which the tunnelling processes contribute to the effective low-energy Hamiltonian is 2. At this order, the tunnelling term leads to two-dimer “plaquette flips” as well as renormalisation of bare onsite potentials  $\mu_i$ ’s due to dimers pivoting out of their positions and back. We always recompute bare potentials  $\mu_i$ ’s to maintain equality up to errors  $O(\epsilon^3)$  among the renormalized  $\tilde{\mu}_i$ ’s. This freedom to engineer the chemical potential landscape to balance kinetic energy is essential to finding our “exactly soluble point” in the model. Before we derive the constraints which we encounter in tuning the ground state manifold (GSM) to  $\bar{\mathcal{V}}_d$ , we must first explain  $\bar{\mathcal{V}}_d$  and how we map it to dimer coverings.

### III. $d$ -ISOTOPY AND ITS LOCAL SUBSPACES

Although we will eventually be considering a system on a lattice, it is useful to begin by defining the Hilbert spaces of interest,  $\bar{V}_d$  and  $V_d$ , in the smooth, lattice-free setting. Consider a compact surface  $Y$  and the set  $S$  of all multiloops<sup>51</sup>  $X \subset Y$ . If  $\partial Y$  (the boundary of  $Y$ ) is non-empty, we fix once and for all a finite set  $P$  of points on  $\partial Y$  with  $X \cap \partial Y = P$ . We assume  $Y$  is oriented but  $X$  should *not* be. There is a large vector space  $\mathbb{C}^S$ , of complex valued functions on  $S$ . We say  $X$  and  $X'$  are *isotopic* ( $X \sim X'$ ) if one may be gradually deformed into the other with, of course, the deformation being the identity on  $\partial Y$  (see Fig. 3).

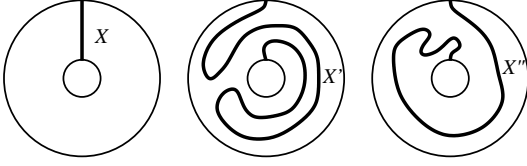


FIG. 3: Isotopy on an annulus:  $X \sim X'$  but  $X \not\sim X''$ .

We may view the isotopy relation as a family of linear constraints on  $\mathbb{C}^S$ , namely  $\Psi(X) - \Psi(X') = 0$  if  $X \sim X'$ . The subspace satisfying these linear constraints is now only of countable dimension; it consists of those functions which depend only of the isotopy class  $[X]$  of  $X$  and may be identified with  $\mathbb{C}^{[S]}$ , where  $[S]$  is the isotopy classes of multiloops with fixed boundary conditions. Note that since all isotopes can be made by composing small locally-supported ones, so the relations we just imposed are “local” in the sense that we will be able to implement them with purely local terms in the Hamiltonian.

Let us go further and define an additional local relation which, when added to isotopy, constitutes the “ $d$ -isotopy” relation. This relation is:

$$d \Psi(X) - \Psi(X \cup \bigcirc) = 0 \quad (2)$$

It says that if two multiloops are identical except for the presence of a small (or, it follows, any contractible) circle, then their function values differ by a factor of  $d$ , a fixed positive real number. In cases of interest to us  $1 \leq d < 2$ , so our function is either neutral to or “likes” small circles. We call the subspace obeying all these constraints the  $d$ -isotopy space of  $Y$  (with fixed boundary conditions) and write it as  $\bar{V}_d \subset \mathbb{C}^{[S]} \subset \mathbb{C}^S$ . The subspace  $\bar{V}_d(T^2)$  is still of countable dimension, or extensively degenerate, on the torus  $T^2$ .

It is a remarkable fact (see Refs. 31,32,36) that it is very difficult to add any further local relations to  $d$ -isotopy without killing the vector space entirely. For  $\alpha$  a root of unity  $\neq \pm 1$ , and  $d = \alpha + \bar{\alpha}$  there is such a local relation, but in almost all cases the natural inner product on  $\bar{V}_d$  fails to be positive definite. The physically interesting cases reduce to  $\alpha = e^{\pi i/(k+2)}$ ,  $k = 1, 2, 3, \dots$ . We call the corresponding  $d$ 's “special”.

In these cases the local relations are essentially the Jones-Wenzl idempotents:

$k = 1$ :

$$\left[ \begin{array}{|c|} \hline \text{---} \\ \hline \end{array} \right] - \frac{1}{d} \left[ \begin{array}{|c|} \hline \text{---} \\ \hline \end{array} \right] = 0 \quad (3)$$

$k = 2$ :

$$\left[ \begin{array}{|c|} \hline \text{---} \\ \hline \end{array} \right] + \frac{1}{d^2 - 1} \left( \left[ \begin{array}{|c|} \hline \text{---} \\ \hline \end{array} \right] + \left[ \begin{array}{|c|} \hline \text{---} \\ \hline \end{array} \right] \right) - \frac{d}{d^2 - 1} \left( \left[ \begin{array}{|c|} \hline \text{---} \\ \hline \end{array} \right] + \left[ \begin{array}{|c|} \hline \text{---} \\ \hline \end{array} \right] \right) = 0 \quad (4)$$

$k = 3$ :

$$\begin{aligned} & \left[ \begin{array}{|c|} \hline \text{---} \\ \hline \end{array} \right] - \frac{d}{d^2 - 2} \left[ \begin{array}{|c|} \hline \text{---} \\ \hline \end{array} \right] - \frac{d^2 - 1}{d^3 - 2d} \left( \left[ \begin{array}{|c|} \hline \text{---} \\ \hline \end{array} \right] + \left[ \begin{array}{|c|} \hline \text{---} \\ \hline \end{array} \right] \right) \\ & + \frac{1}{d^2 - 2} \left( \left[ \begin{array}{|c|} \hline \text{---} \\ \hline \end{array} \right] + \left[ \begin{array}{|c|} \hline \text{---} \\ \hline \end{array} \right] + \left[ \begin{array}{|c|} \hline \text{---} \\ \hline \end{array} \right] + \left[ \begin{array}{|c|} \hline \text{---} \\ \hline \end{array} \right] \right) \\ & - \frac{1}{d^3 - 2d} \left( \left[ \begin{array}{|c|} \hline \text{---} \\ \hline \end{array} \right] + \left[ \begin{array}{|c|} \hline \text{---} \\ \hline \end{array} \right] \right) + \frac{d^2}{d^4 - 3d^2 + 2} \left[ \begin{array}{|c|} \hline \text{---} \\ \hline \end{array} \right] \\ & - \frac{d}{d^4 - 3d^2 + 2} \left( \left[ \begin{array}{|c|} \hline \text{---} \\ \hline \end{array} \right] + \left[ \begin{array}{|c|} \hline \text{---} \\ \hline \end{array} \right] \right) + \frac{1}{d^4 - 3d^2 + 2} \left[ \begin{array}{|c|} \hline \text{---} \\ \hline \end{array} \right] \\ & = 0, \quad (5) \end{aligned}$$

see Ref. 30 for a recursive formula. These relations define a finite dimensional Hilbert space  $V_d(Y) \subset \bar{V}_d(Y) \subset \mathbb{C}^{[S]} \subset \mathbb{C}^S$ .

In Refs. 31,32 it is explained that these  $V_d(Y)$  are the Hilbert space for  $\mathcal{DK}_k$  mentioned earlier,  $d = 2 \cos \pi/(k+2)$ . It is argued that a Hamiltonian with GSM corresponding to  $\bar{V}_d$  may be unstable and collapse under perturbation (for  $k = 1$  or 2 and under a larger deformation for  $k \geq 3$ ) to  $V_d$ . Very briefly, TQFTs such as  $\mathcal{DK}_k$ , can always be defined as the joint null space of commuting local projectors<sup>52</sup>, implying the existence of a local Hamiltonian with a spectral gap in the thermodynamic limit. Once a Hamiltonian  $H_d$  has imposed  $d$ -isotopy, i.e.  $GSM(H_d) = \bar{V}_d$ , an extensive degeneracy has been created; the only local way of lifting this extensive degeneracy (to a finite degeneracy) without creating frustration<sup>53</sup> is to impose the Jones-Wenzl projector as a constraint. Although frustration may arise in a Hamiltonian describing a topological phase, we know that these phases can be produced by an unfrustrated Hamiltonian. Thus it is an attractive ansatz that near  $H_d$  will be some  $H_{d,\epsilon}$  with  $GSM(H_{d,\epsilon}) = V_d$ .

To this point our discussion has contemplated smooth multiloops  $X$  on a surface  $Y$ ; now it is appropriate to move to a lattice setting. It is an old idea (see e.g. Ref. 37) to turn a dimerization (perfect matching)  $\mathcal{J}$  into a multiloop  $\mathcal{R} \cup \mathcal{J}$  by using a background dimerization  $\mathcal{R}$  to form a ‘transition graph’. If the lattice  $\mathcal{L}$  is bipartite then  $\mathcal{R} \cup \mathcal{J}$  can be oriented in a natural way, leading to conserved quantities<sup>54</sup> – integral winding numbers – which are disrespected by the Jones-Wenzl (JW) relations. For this reason we pass over the square and hexagonal lattices as poor candidates for the imposition of the JW relations crucial to the passage from  $\bar{V}_d$  to  $V_d$ . Thus we consider perfect matchings on the triangular lattice  $\mathcal{T}$ . By fixing

$\mathcal{R}$  as in Fig. 2, without small rhombi with two opposite sides red, as the preferred background dimerization we obtain the fewest equations in defining  $\bar{V}_d$  and also achieve ergodicity<sup>55</sup> under a small set of moves. Unlike in the usual case, the background dimerization,  $\mathcal{R}$ , is not merely a guide for the eyes, but will be *physically* distinguished: the chemical potentials and tunnelling amplitudes will be different for bonds of different color.

Let us list here the elementary dimer moves that preserve the proper dimer covering condition:

- **Plaquette (rhombus) flip** – this is a two-dimer move around a rhombus made of two lattice triangles. Depending on whether a “red” bond forms a side of such a rhombus, its diagonal, or is not found there at all, the plaquettes are referred to, respectively, as type 1 (or 1’), 2, or 3 (see Fig. 4). The distinction between plaquettes of type 1 and 1’ is purely directional: diagonal bonds in plaquettes of type 1 are horizontal, for type 1’ they are not. This distinction is necessary since our Hamiltonian breaks the rotational symmetry of a triangular (or Kagomé) lattice.
- **Triangle move** – this is a three-dimer move around a triangle made of four elementary triangles. One such “flippable” triangle is labelled 4 in Fig. 4.
- **Bow tie move** – this is a four-dimer move around a “bow tie” made of six elementary triangles. One such “flippable” bow tie is labelled 5 in Fig. 4.

To make each of the above moves possible, the actual dimers and unoccupied bonds should alternate around a corresponding shape. Notice that for both triangle and bow tie moves we chose to depict the cases when the maximal possible number of “red” bonds participate in their making (2 and 4 respectively).

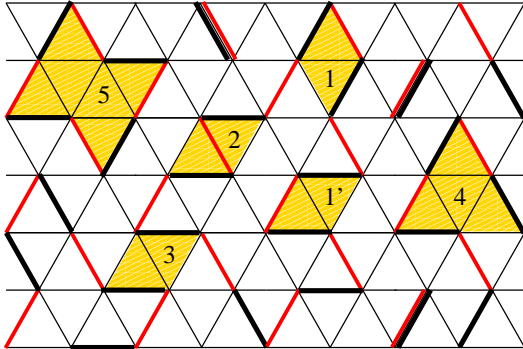


FIG. 4: Overlap of a dimer covering of  $\mathcal{T}$  (shown in thick black) with the red covering corresponding to the special sublattice  $\mathcal{R}$ . Shaded plaquettes correspond to various dimer moves described in the text. Green sublattice is not shown.

Note that there are no alternating red/black rings of fewer than 8 lattice bonds (occupied by at most 4 non-colliding dimers). Ring moves only occur when red and black dimers alternate; the triangle labelled 4 in Fig. 4 does not have a Ring term associated with it, but the bow tie labelled 5 does.

Here is the correspondence between the previous smooth discussion and rhombus flips relating dimerizations  $\mathcal{J}$  of  $\mathcal{T}$ . The surface  $Y$  is now a planar domain or possibly a torus (periodic boundary conditions). A multiloop  $X$  in  $Y$  becomes  $X = \mathcal{R} \cup \mathcal{J}$  (with the convention that the dimers of  $\mathcal{R} \cap \mathcal{J}$  be considered as length 2 loops or bigons). What about isotopy? Move (2) certainly is an isotopy from  $\mathcal{R} \cup \mathcal{J}$  to  $\mathcal{R} \cup \mathcal{J}'$  but move (2), by itself, does almost nothing. It is not possible to build up long motions from (2) alone. So it is a peculiarity of the rhombus flips that we have no good analog of isotopy alone but instead go directly to  $d$ -isotopy. Move (1) must be considered in two different forms (1) and (1’) as a result of the color differences (see Fig. 4). The reader may expect us to impose the relations associated with type (5) and (1), (1’) moves:

$$d^3 \Psi \left( \begin{array}{c} \text{Rhombus flip (1)} \end{array} \right) - \Psi \left( \begin{array}{c} \text{Rhombus flip (1')} \end{array} \right) = 0, \quad (6a)$$

$$d \Psi \left( \begin{array}{c} \text{Triangle move (4)} \end{array} \right) - \Psi \left( \begin{array}{c} \text{Triangle move (4')} \end{array} \right) = 0 \quad (6b)$$

since we pass from one to four loops in (6a) and zero to one loop in (6b).

However, by choosing, instead a less obvious mapping of  $\bar{V}_d$  to functions on  $\{\mathcal{J}\}$  we end up imposing one fewer equation on the Hubbard parameters. So instead we impose:

$$b \Psi \left( \begin{array}{c} \text{Rhombus flip (1)} \end{array} \right) - \Psi \left( \begin{array}{c} \text{Rhombus flip (1')} \end{array} \right) = 0, \quad (7a)$$

$$a \Psi \left( \begin{array}{c} \text{Triangle move (4)} \end{array} \right) - \Psi \left( \begin{array}{c} \text{Triangle move (4')} \end{array} \right) = 0 \quad (7b)$$

and require that  $a^4/b = d$ .

In other words, the two processes, (1) and (1’) for making length 2 loops and the one process (5) for fusing four length 2 loops in one loop of length 8 (see Fig. 4) will have to be tuned to satisfy Eqs. (7) and  $a^4/b = d$ .

Given  $\Psi \in \bar{V}_d$ , let  $\Psi_\rho(\mathcal{J}) = a^\# \Psi((\mathcal{R} \cup \mathcal{J})^-)$  where  $\#$  is the number of length 2 loops of  $\mathcal{R} \cup \mathcal{J}$  (i.e.  $\#$  of dimers common to  $\mathcal{R}$  and  $\mathcal{J}$ ) and  $(\mathcal{R} \cup \mathcal{J})^-$  is the multiloop  $\mathcal{R} \cup \mathcal{J} \setminus \mathcal{R} \cap \mathcal{J}$ , i.e. all of the loops except the length 2 loops. This pulls  $\Psi$ , a function on multiloops back to a function  $\Psi_\rho(\mathcal{J})$  on dimerizations. If  $\mathcal{J}$  and  $\mathcal{J}'$  are linked by finitely many applications of Eqs. (7) and the isotopy move, it is now easy to check that  $\Psi_\rho(\mathcal{J}) = a^{(\#-\#')} d^{(c'-c)} \Psi_\rho(\mathcal{J}')$  where  $c$  (resp.  $c'$ ) is the number of non-essential loops of length exceeding two in  $\mathcal{R} \cup \mathcal{J}$  (resp.  $\mathcal{R} \cup \mathcal{J}'$ ).

This separate accounting for length 2 loops and the longer circles may appear to be a slight of hand. Is there a price to pay? In a sense, yes: It is now crucial that a combinatorial relation which mimics the smooth JW relation by relating  $(\mathcal{J}_1, \mathcal{J}_2)$  for  $k = 1, (\mathcal{J}_1, \dots, \mathcal{J}_5)$  for level 2,  $(\mathcal{J}_1, \dots, \mathcal{J}_{14})$  for level 3, etc... must not in any of its terms change the number of length 2 loops. But this is just an additional (and readily achieved) condition on the combinatorial form of the JW projector and does not influence the algebraic conclusion: that (only) for special  $d$  is there a unfrustrated local reduction  $V_d \subset \bar{V}_d$  which could be a stable phase and when  $d$  is special

$V_d$  is unique. Thus the combinatorial analog of  $\bar{V}_d$  is functions on  $\{\mathcal{J}\}$  obeying Eqs. (7) with  $a^4/b = d$ .

#### IV. THE ANALYSIS OF $A$ AND $A^-$

In this section we derive the effective Hamiltonian  $\tilde{H} : \mathcal{D} \rightarrow \mathcal{D}$  on the span of dimerizations. The derivation is perturbative to the second order in  $\varepsilon$  where  $\varepsilon = t_{bb}^r/U = t_{gb}^b/U$ . Additionally,  $t_{rb}^b/U = c_0\varepsilon$  where  $c_0$  is a positive constant, while  $t_{bb}^g = o(\varepsilon)$  and can be neglected in the second-order calculations. (In the absence of a magnetic field all  $t$ 's can be made real and hence symmetric with respect to their lower indices. Also, from now on we set  $U = 1$  for notational convenience.)

As explained in Section III, we then shall tune  $\tilde{H}$  to the ‘‘small loop’’ value  $a$  and the ‘‘bow tie’’ value  $b$  with  $a^4/b = d$ .

We account for all second-order processes, i.e. those processes that take us out of  $\mathcal{D}$  and then back to  $\mathcal{D}$  (see Appendix B for technical details). As mentioned earlier, these amount to off-diagonal (hopping) processes – ‘‘plaquette’’ flips’’ or ‘‘rhombus moves’’ – as well as diagonal ones (potential energy) in which a dimer pivots out and then back into its original position. The latter processes lead to renormalisation of the bare onsite potentials  $\mu_i$ , which we have adjusted so that all renormalised potentials  $\tilde{\mu}_i$  are equal up to corrections  $O(\varepsilon^3)$ . The non-constant part of the effective Hamiltonian comes from the former processes and can be written in the form:

$$\tilde{H} = \sum_{I,J} (\tilde{H}_{IJ} \otimes \mathbb{I}) \tilde{\delta}_{IJ} \quad (8)$$

where  $\tilde{H}_{IJ}$  is a  $2 \times 2$  matrix corresponding to a dimer move in the two-dimensional basis of dimer configurations connected by this move.  $\tilde{\delta}_{IJ} = 1$  if the dimerizations  $I, J \in \mathcal{D}$  are connected by an allowed move,  $\tilde{\delta}_{IJ} = 0$  otherwise.

Therefore it suffices to specify these  $2 \times 2$  matrices  $\tilde{H}_{IJ}$  for the off-diagonal processes. For moves of types (1)-(3), these matrices are given below. Type (1), e.g. rhombus (VY) in Fig. 5:

$$\begin{pmatrix} v_{gb}^b & -2t_{rb}^b t_{gb}^b \\ -2t_{rb}^b t_{gb}^b & v_{rb}^b \end{pmatrix} = \begin{pmatrix} v_{gb}^b & -2c_0\varepsilon^2 \\ -2c_0\varepsilon^2 & v_{rb}^b \end{pmatrix} \sim \begin{pmatrix} a & -1 \\ -1 & a^{-1} \end{pmatrix} \quad (9)$$

Type (1'), e.g. rhombus (VW) in Fig. 5:

$$\begin{pmatrix} v_{bb}^b & -2t_{rb}^b t_{gb}^b \\ -2t_{rb}^b t_{gb}^b & v_{rg}^b \end{pmatrix} = \begin{pmatrix} v_{bb}^b & -2c_0\varepsilon^2 \\ -2c_0\varepsilon^2 & v_{rb}^b \end{pmatrix} \sim \begin{pmatrix} a & -1 \\ -1 & a^{-1} \end{pmatrix} \quad (10)$$

Type (2), e.g. rhombus (UV) in Fig. 5:

$$\begin{pmatrix} v_{bb}^r & -2(t_{bb}^r)^2 \\ -2(t_{bb}^r)^2 & v_{bb}^r \end{pmatrix} = \begin{pmatrix} v_{bb}^r & -2\varepsilon^2 \\ -2\varepsilon^2 & v_{bb}^r \end{pmatrix} \sim \begin{pmatrix} 1 & -1 \\ -1 & 1 \end{pmatrix} \quad (11)$$

since isotopic multiloops should have equal weights.

Finally, type (3), e.g. rhombus (WX) in Fig. 5:

$$\begin{pmatrix} v_{bb}^g & -2(t_{bb}^g)^2 \\ -2(t_{bb}^g)^2 & v_{bb}^g \end{pmatrix} = \begin{pmatrix} v_{bb}^g & 0 \\ 0 & v_{bb}^g \end{pmatrix} = \begin{pmatrix} 0 & 0 \\ 0 & 0 \end{pmatrix}, \quad (12)$$

provided  $k > 1$ , since it represents a ‘‘surgery’’ similar to Eq. (3). (For  $k = 1$ , on the other hand, this matrix must be proportional to  $\begin{pmatrix} 1 & -1 \\ -1 & 1 \end{pmatrix}$ .) As follows from Eq. (3), at level  $k = 1$  multiloops which differ by a surgery should have equal coefficients in any ground state vector  $\Psi$  while at levels  $k > 1$  no such relation should be imposed. We use the symbol ‘‘ $\sim$ ’’ to denote proportional via a positive factor.

The matrix relations (9-12) yield equations in the model parameters (we consider now only the case  $k > 1$ ):

$$\text{Types (1)\&(1')} : \quad v_{gb}^b = v_{bb}^b = 2ac_0\varepsilon^2 \quad (13a)$$

$$\text{and } v_{rb}^b = v_{rg}^b = 2a^{-1}c_0\varepsilon^2 \quad (13b)$$

$$\text{Type (2)} : \quad v_{bb}^r = 2\varepsilon^2 \quad (13c)$$

$$\text{Type (3)} : \quad v_{bb}^g = 0 \quad (13d)$$

We suppose that the Hamiltonian has a bare ring exchange term, Ring in Eq. (1):  $\text{Ring} = \begin{pmatrix} x & -c_3\varepsilon^2 \\ -c_3\varepsilon^2 & y \end{pmatrix}$  for some constants  $c_3, x, y > 0$ , and consider the additional equations which come from considering Ring as a fluctuation between one loop of length 8 (labelled (5) in Fig. 4) and four loops of length 2. It follows from Eq. (7a) that  $\text{Ring} \sim \begin{pmatrix} b & -1 \\ -1 & 1/b \end{pmatrix}, b > 0$  so:

$$a^4/b = d, \quad x/\varepsilon^2 = bc_3, \quad y/\varepsilon^2 = b^{-1}c_3. \quad (14)$$

are the additional equations (beyond Eqs. (13)) to place model  $A$  at the soluble point  $\bar{V}_d$ . The justification of the diagonal entries in the ring term is that the 4 particles in  $\Psi_0$  and  $\Psi_1$  form a square which has some cost over an ideal Winger crystal of particles. This cost can be influenced by the local chemical environment so the entries do not need to be equal, though  $x = y$  is the most natural case.

Computer studies<sup>38</sup> show that with the Ring term present all  $\mathcal{J}$  are connected by repeated application of the Hamiltonian (and respect the  $d$ -isotopy relation). When the Ring term is removed, it still appears that any two dimerizations  $\mathcal{J}$  and  $\mathcal{J}'$  which determine isotopic loops nesting patterns  $(\mathcal{R} \cup \mathcal{J})$  and  $(\mathcal{R} \cup \mathcal{J}')$  (use our conversion to consider bigons as loops) communicate. So, e.g., in a disk if  $\mathcal{R} \cup \mathcal{J}$  and  $\mathcal{R} \cup \mathcal{J}'$  have the same number of loops and the same combinatorial nesting relations, and if  $\mathcal{R}, \mathcal{J}$ , and  $\mathcal{J}'$  all agree near the disk boundary, then moves of type (1), (1'), (2), and their reversals will connect  $\mathcal{J}$  and  $\mathcal{J}'$ . Since the Jones-Wenzl relations do violence to

the nesting patterns it is hard to imagine any *additional* conserved quantities which could allow the ground state *without* the Ring term to collapse to a richer (more degenerate) topological phase than  $\mathcal{DK}_k$  itself (for some  $k$ ). So we suspect that the Ring term is redundant if the goal is to arrive in a topological phase.

However, there is a caution which should be issued if the ring term is omitted. Because of the possibility of defining a separate circle value  $a$  for bigons and a value  $b$  for breaking 8-gons, with only the relation  $\frac{a^4}{b} = d$  tying the model to a fixed level<sup>56</sup> the  $A^-$  model (Eq. (1) with Ring omitted) could still be tuned to any level  $k$  because only  $a$  and not  $b$  has been given. Thus, for example  $\mathcal{DK}_1$  can still arise if an effective Ring term with  $b = a^4$  emerges.

But, as we have remarked, physically it is most natural to assume  $x = y$  in the Ring term. This forces  $b = 1$  and  $a = d^{1/4}$ . Note that we do *not* want fluctuations on the alternating green-black 8-bond rings as this would mix distinct topological sectors and no such terms are in the Hamiltonian (1).

Our simplest bosonic candidate for a “universal quantum computer” would be model  $A$  tuned to  $a = \left(\frac{1+\sqrt{5}}{2}\right)^{1/4}$ ;  $x = y = c_3 \varepsilon^2$  in Ring (and no green-black Ring term).

## V. MODEL $B$ (SPINLESS BOSON/NO RING TERM)

For this model we work entirely within the extended Hubbard model,  $H$ , as in Eq. (1) with no Ring term. What replaces the 4-particle ring exchange term is a flip of a new rhombus of type  $(r, r)$ :  (e.g. rhombus  $QP$  in Fig. 5) which can be interpreted as an alternating ring of length 4. We create an extensive system of (for example, bi-periodic) “defects” in the red sublattice  $\mathcal{R}$ . A defect is made by rotating four red edges by a  $1/8$ -turn around a bow tie. Inspecting this defect reveals two  $(r, r)$ -rhombi adjacent to the defect. The required  $(r, r)$ -rhombus flip can easily be coaxed out of the Hubbard model at  $O(\varepsilon^2)$  so there is no need to include an ad hoc Ring term. (Without a defect a Ring term does not arise until order  $O(\varepsilon^4)$  – see Appendix B.)

We can construct a  $d$ -isotopy space  $\bar{V}_d$  as the GSM of model  $B$  in a similar fashion to model  $A^-$ , but the price of having introduced the defect is that there are now many more exceptional cases for type (1), (2), and (3) moves. A proliferation of colors must be defined so that raw potentials  $\mu_i$  when renormalized by hopping in all the different local environments come out equal up to  $O(\varepsilon^2)$ . We introduce the colors (see Fig. 5):  $g$ (green),  $b$ (black),  $i$ (indigo),  $r$ (red),  $l$ (lavender), and  $G$ (thick green),  $B$ (thick black) which are identical in tunnelling properties to  $g$  and  $b$  (resp.) but require different on-site potentials  $\mu_G \neq \mu_g$  and  $\mu_B \neq \mu_b$ .

We take the following relations (which are not the most

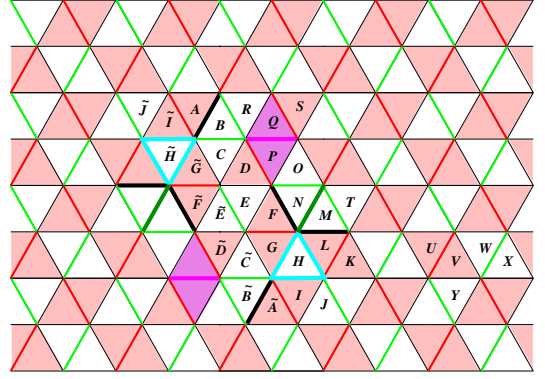


FIG. 5: Sublattice defect, a single bow tie rotation of  $\mathcal{R}$ , in bosonic model  $B$ . Two rhombi with alternating red and black edges (type  $(r, r)$ ) are shaded lavender. Triangles forming plaquettes whose color environment is affected by the defect are labelled  $A - T$  and  $\tilde{A} - \tilde{T}$  (with notations reflecting the obvious inversion symmetry). Triangles labelled  $U - Y$  form regular plaquettes.

general possible):

$$0 = t_{bb}^g = t_{gb}^g = t_{gb}^G = t_{Gb}^g \quad (15a)$$

$$\varepsilon = t_{bb}^r = t_{gb}^b = t_{bl}^r = t_{il}^i = t_{lr}^r = t_{gg}^b = t_{gG}^b \quad (15b)$$

$$c_0 \varepsilon = t_{lr}^b = t_{ir}^b = t_{br}^x = t_{bb}^l, \quad \text{for } x \neq l \quad (15c)$$

$$c_1 \varepsilon = t_{br}^l \quad (15d)$$

(Note: With regard to tunnelling amplitudes,  $i$  behaves like  $b$  except  $t_{ii}^i = \varepsilon$  which has no  $b$ -analog.)

Near the defect in  $\mathcal{R}$  many special rhombi occur and must be considered. All labelled rhombi (those bearing two letters in Fig. 5) can be classified by the topological effect of a two-dimer move: types (1) and (1') create or absorb a loop of length 2, type (2) is an isotopy move, type (3) is a surgery and an additional type  $(r, r)$  (e.g. rhombus  $(QP)$ ) breaks a 4-gon into two bigons (or the reverse). Regard the interaction potentials  $v$  as variables and for each labelled rhombus write the matrix relations, extending Eqs. (9)–(12). we may now solve for the  $v$ 's as functions of the  $t$ 's as shown below (16–17). To shorten the list of  $v$ 's we assume that capitalisation of indices for  $v$  has no effect. Similarly, we assume that  $i$  and  $b$  are interchangeable.

$$\text{Type (3):} \quad 0 = v_{bb}^g = v_{bg}^g \quad (16a)$$

$$\text{Type (2):} \quad 2\varepsilon^2 = v_{bb}^r = v_{bl}^r \quad (16b)$$

$$\text{Types (1)\&(1')}: \quad 2ac_0\varepsilon^2 = v_{gb}^b = v_{bb}^b = v_{bi}^b = v_{ib}^b \quad (16c)$$

$$\text{and} \quad 2a^{-1}c_0\varepsilon^2 = v_{rb}^b = v_{rg}^b \quad (16d)$$

The only relation not previously appearing in model  $A^-$  comes from from type  $(r, r)$  rhombi (e.g.  $(QP)$ ):

$$\begin{pmatrix} v_{bb}^l & -2(t_{rb}^l)^2 \\ -2(t_{rb}^l)^2 & v_{rr}^l \end{pmatrix} \sim \begin{pmatrix} b & -1 \\ -1 & b^{-1} \end{pmatrix} \\ \Rightarrow v_{bb}^l = 2bc_1^2\varepsilon^2, \quad v_{rr}^l = 2b^{-1}c_1^2\varepsilon^2, \quad (17)$$

with the additional constraint  $a^2/b = d$ .

In principle, all labelled rhombi give relations on  $v$ 's as functions of the  $t$ 's, but we have set things up so that these further relations are redundant with the ones coming from  $VY$ ,  $VW$ ,  $UV$ ,  $WX$  and  $QP$  which we have already used in deriving (16-17). In the following table we begin a verification which the reader may complete.

Type (1'), rhombus ( $\tilde{I}$ ):

$$\begin{pmatrix} v_{ib}^b & -2t_{gb}^b t_{ri}^b \\ -2t_{gb}^b t_{ri}^b & v_{rg}^b \end{pmatrix} \Rightarrow t_{ri}^b = c_0 \epsilon, v_{ib}^b = v_{bb}^b \quad (18)$$

Type (2), rhombus ( $\tilde{I}A$ ):

$$\begin{pmatrix} v_{ib}^r & -2(t_{bb}^r)^2 \\ -2(t_{bb}^r)^2 & v_{Bb}^r \end{pmatrix} \Rightarrow v_{ib}^r = v_{bb}^r, v_{Bb}^r = v_{bb}^r, t_{bb}^r = \epsilon \quad (19)$$

Type (1'), rhombus ( $AB$ ):

$$\begin{pmatrix} v_{bg}^B & -2t_{gg}^B t_{rb}^B \\ -2t_{gg}^B t_{rb}^B & v_{rg}^B \end{pmatrix} \Rightarrow t_{rb}^B = c_0 \epsilon, t_{gg}^B = \epsilon, v_{bg}^B = v_{bg}^b, v_{gr}^B = v_{gr}^b \quad (20)$$

## VI. FERMIONIC MODELS C AND D

For  $C$  the Hamiltonian is again (1) but with  $c_i$  and  $c_1^\dagger$  spinless fermionic annihilation and creation and operators. The lattice will be triangular  $\mathcal{T}$ . The special background dimerization will be the red sublattice  $\mathcal{R}$ . The green sublattice  $\mathcal{G}$  is also marked and edges of  $\mathcal{B} := \mathcal{T} \setminus (\mathcal{R} \cup \mathcal{G})$  will be called black, see Fig. 2.

The main difference from model  $A$  is that we introduce ‘‘indirect’’ hopping between adjacent edges which are *angle insensitive*. We regard the vertices of  $\mathcal{T}$  as additional *virtual* sites at a higher chemical potential through which a particle can hop. The benefit is that the type 3 move becomes symmetric: the  $60^\circ$ ,  $60^\circ$  hops cancel the  $120^\circ$ ,  $120^\circ$  hops. We also must include some ‘‘direct’’,  $60^\circ$  only, hopping terms to avoid killing the desired processes 1 and 2. Here are the tunnelling amplitudes (again setting  $U = 1$ ).

indirect: There will be a tunnelling amplitude  $t$  between any two edges of  $\mathcal{T}$  which share a vertex (regardless of color or angle)  $t = \epsilon$ .

direct:  $t_{bb}^g = 0$ ,  $t_{rb}^b = c_1 \epsilon$ ,  $t_{gb}^b = c_2 \epsilon$ ,  $t_{bb}^r = c_3 \epsilon$ .

Ring term:  $\begin{pmatrix} c_4 b \epsilon^2 & -c_4 \epsilon^2 \\ -c_4 \epsilon^2 & c_4 b^{-1} \epsilon^2 \end{pmatrix}$ .

Here are the terms in the Hamiltonian  $H$  and the corresponding equations:

Type (1):

$$\begin{pmatrix} v_{gb}^b & -2c_1 c_2 \epsilon^2 \\ -2c_1 c_2 \epsilon^2 & v_{rb}^b \end{pmatrix} \sim \begin{pmatrix} a & -1 \\ -1 & a^{-1} \end{pmatrix} \quad (21)$$

Type (1'):

$$\begin{pmatrix} v_{bb}^b & -2c_1 c_2 \epsilon^2 \\ -2c_1 c_2 \epsilon^2 & v_{rb}^b \end{pmatrix} \sim \begin{pmatrix} a & -1 \\ -1 & a^{-1} \end{pmatrix} \quad (22)$$

Type (2):

$$\begin{pmatrix} v_{bb}^r & \begin{matrix} (\text{dir dir}) & (\text{dir ind}) & (\text{ind ind}) \\ -2c_2^2 \epsilon^2 & -4c_2 \epsilon^2 & -0 \end{matrix} \\ -2c_2^2 \epsilon^2 - 4c_2 \epsilon^2 & v_{bb}^r \end{pmatrix} \sim \begin{pmatrix} 1 & -1 \\ -1 & 1 \end{pmatrix} \quad (23)$$

Type (3):

$$\begin{pmatrix} v_{bb}^g & 0 \\ 0 & v_{bb}^g \end{pmatrix} = \begin{pmatrix} 0 & 0 \\ 0 & 0 \end{pmatrix} \quad (24)$$

Type (5):

$$\text{Ring} \sim \begin{pmatrix} bc_4 \epsilon^2 & -c_4 \epsilon^2 \\ -c_4 \epsilon^2 & b^{-1} c_4 \epsilon^2 \end{pmatrix} \quad (25)$$

We must therefore impose the following equations:

$$\begin{aligned} & a^4/b = d \\ (2) : & v_{bb}^r = (2c_2^2 + 4c_2) \epsilon^2 \\ (1) \text{ and } (1') : & v_{gb}^b = v_{bb}^b = 2ac_1 c_2 \epsilon^2 \\ & \text{and } v_{rb}^b = v_{rg}^b = 2a^{-1} c_1 c_2 \epsilon^2 \\ (3) : & v_{bb}^g = 0 \end{aligned} \quad (26)$$

As in bosonic models, the required potentials can be solved for from the tunnelling amplitudes.

As with model  $A$ , we may simply omit the Ring term from model  $C$  to get model  $C^-$ . Under the assumption that an effective ring term with  $b = 1$  emerges,  $C^-$  could be tuned to yield  $\mathcal{DK}_k$ .

Finally we treat model  $D$ . We use the same  $\mathcal{R}$ , red sublattice *with* defects as in model  $B$ . The necessary colorings are illustrated in Fig. 6.

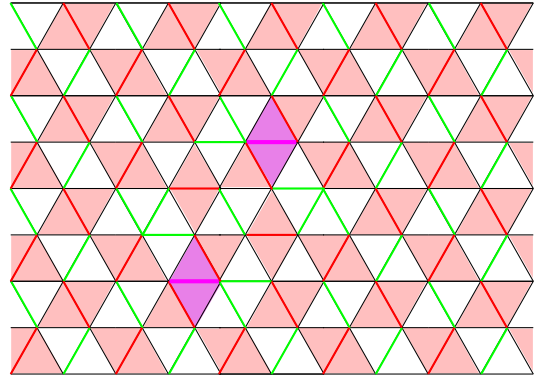


FIG. 6: Sublattice defect in fermionic model  $D$ .

We list the tunnelling amplitudes:

indirect:  $t = \epsilon$  between all adjacent edges,  $e_i \cap e_j \neq \emptyset$ .

direct:

$$0 = t_{bb}^g = t_{gb}^g \quad (27a)$$

$$c_1 \epsilon = t_{rb}^b = t_{lb}^b \quad (27b)$$

$$c_2 \epsilon = t_{gb}^b = t_{gg}^b \quad (27c)$$

$$c_3 \epsilon = t_{bb}^r = t_{lb}^r \quad (27d)$$

$$c_4 \epsilon = t_{rb}^l \quad (27e)$$

We have only listed colors  $b, r, g, l$  but some of these may appear in two or three forms because of differing local environment. Though each of these forms needs an individual  $\mu$  (chemical potential), the  $t$  and  $v$  symbols will depend only on the 4 given colors.

Near the defect, to maintain the equations of model  $A$  we need to set:  $v_{gb}^g = v_{bb}^g, v_{bl}^r = v_{bb}^r, v_{gl}^b = v_{gb}^b, v_{rl}^b = v_{rb}^b, v_{lb}^b = v_{bb}^b$ .

This effectively maintains the constraints associated to rhombi of types 1, 1', 2, and 3 near the defect.

The lavender rhombi (Fig. 6) yield a new term which must be constrained by the equations below.

$$\begin{pmatrix} v_{bb}^l & -2c_4^2 \epsilon^2 \\ -2c_4^2 \epsilon^2 & v_{rr}^l \end{pmatrix} \sim \begin{pmatrix} b & -1 \\ -1 & b^{-1} \end{pmatrix}, \quad \frac{a^2}{b} = d \quad (28)$$

so we have the equations:

$$v_{bb}^l = 2bc_4^2 \epsilon^2, \quad v_{rr}^l = 2b^{-1}c_4^2 \epsilon^2, \quad \frac{a^2}{b} = d, \quad (29)$$

in addition to the equation from model  $C$ :

$$v_{bl}^r = v_{bb}^b = (2c_2^2 + 4c_2) \epsilon^2 \quad (30a)$$

$$v_{gl}^b = v_{gb}^b = v_{bb}^b = 2ac_1c_2 \epsilon^2 \quad (30b)$$

$$v_{rl}^b = v_{rb}^b = 2a^{-1}c_1c_2 \epsilon^2 \quad (30c)$$

$$v_{gb}^g = v_{bb}^g = 0. \quad (30d)$$

To find solutions it is only necessary to choose  $a$  and  $b$  compatible, pick the positive constants  $c_1, \dots, c_4$  and compute the potentials  $v$ .

### Acknowledgments

The authors would like to thank D. Jethchev for kindly providing a computer program for exploring dimer dynamics and K. Walker for his help in automated diagrammatic calculation of the Jones-Wenzl projectors reproduced in section III. The authors would also like to thank S. Kivelson, S. Sondhi, K. Walker, and Z. Wang for helpful discussion and the Aspen Center for Physics where a part of this paper was completed for its hospitality. C.N. acknowledges the support of the National Science foundation under grant DMR-9983544 and the Alfred P. Sloan Foundation.

### APPENDIX A: DEFINITION AND PROPERTIES OF $\mathcal{DK}_k$

The information in this appendix allows one to predict the outcome of any Aharonov-Bohm experiment conducted on a material thought to be in the topological phase  $\mathcal{DK}_k$ .

There is a well known<sup>39</sup> family of topological quantum field theories (TQFTs)  $SU(2)_k$ . These are the unitary  $SU(2)$  TQFTs at level  $k$ . In the quantum group approach<sup>40</sup> in order to define precisely this theory (and not e.g. its time reverse) one sets the deformation parameter  $A$  for the universal enveloping algebra of  $su(2)$  to  $A = e^{2\pi i/4(k+2)}$ .

$SU(2)_k$  has particles species indexed by  $SU(2)$  representations (or 'isospins')  $j = 0, 1/2, 1, \dots, k/2$ . These  $k+1$  irreducible representations are subject to the following rules:

The fusion space  $V_{j_1 j_2}^{j_3} \cong C$  if

$$0 \leq j_1, j_2, j_3, \leq k/2 \quad (A1a)$$

$$j_1 + j_2 \geq j_3, \quad (A1b)$$

$$j_3 + j_1 \geq j_2, \quad (A1c)$$

$$j_2 + j_3 \geq j_1, \quad (A1d)$$

$$j_1 + j_2 + j_3 \leq k. \quad (A1e)$$

$\cong 0$  otherwise.

The  $S$ -matrix is

$$S_{j_1 j_2} = \sqrt{\frac{2}{k+2}} (\sin(2j_1 + 1)(2j_2 + 1)\pi/(k+2)), \quad 0 < i, j \leq k/2. \quad (A2)$$

There is a variant  $K_k$  of  $SU(2)_k$  worked out in<sup>41</sup> (also see Refs. 32,36) based on the Kauffman bracket for links but now with  $A = ie^{2\pi i/4(k+2)}$  in the relation of Fig. 7.

$$\begin{array}{c} \diagup \quad \diagdown \\ \diagdown \quad \diagup \end{array} = A \left( \begin{array}{c} + \\ - \end{array} \right) \left( \begin{array}{c} \cup \\ \cap \end{array} \right)$$

FIG. 7: Kauffman bracket

On a torus  $T^2$ ,  $K_k(T^2)$  would be a subspace of the functions on links in the *solid* torus, respecting the above relation, the level  $k$  Jones-Wenzl relation, small unknots  $= d = 2 \cos \pi/k + 2$ , and finally the relation that a right handed kink is equal  $-A^{-3}$ .  $K_k$  also has  $k+1$  orthogonal irreps  $0, \dots, k$  with the same fusion relations as  $SU(2)_k$  but the  $S$ -matrix is  $\tilde{S}_{j_1 j_2} = (-1)^{4j_1 j_2} \sqrt{\frac{2}{k+2}} (\sin(2j_1 + 1)(2j_2 + 1)\pi/(k+2))$ .

$K_k$  is a Chern-Simons-Higgs theory in which two  $SU(2)$  Chern-Simons gauge fields, with levels  $k$  and 1, are tied together by a condensate which transforms in the isospin  $k/2$  representation of the first and the isospin  $1/2$  representation of the second:

$$\mathcal{S} = k\mathcal{S}_{CS}[a_1] - \mathcal{S}_{CS}[a_2] + \mathcal{S}_{\text{Higgs}}[\Phi, a_1, a_2] \quad (A3)$$

where

$$\begin{aligned} \mathcal{S}_{CS} &= \frac{1}{4\pi} \int \epsilon^{\mu\nu\rho} \left( a_\mu^a \partial_\nu a_\rho^a + \frac{2}{3} f_{abc} a_\mu^a a_\nu^b a_\rho^c \right) \\ &= \frac{1}{4\pi} \int \text{tr} \left( a \wedge da + \frac{2}{3} a \wedge a \wedge a \right) \end{aligned} \quad (A4)$$

and

$$\mathcal{S}_{\text{Higgs}}[\Phi, a_1, a_2] = \int \left| \left( i\partial_\mu + a_{1\mu}^a T_{IJ}^a + a_{2\mu}^a t_{ij}^a \right) \Phi_{Jj} \right|^2 + V(\Phi) \quad (A5)$$

$\underline{a} = 1, 2, 3$  are  $su(2)$  Lie algebra indices;  $T^a, t^a$  are  $su(2)$  generators in the isospin  $k/2$  and  $1/2$  representations, respectively.  $V(\Phi)$  is minimized at non-zero  $|\Phi|$ . The presence of

the condensate restricts the possible particle types so that half-integer isospins under  $SU(2)_k$  are necessarily spin-1/2 under  $SU(2)_1$ . This leads to the additional minus signs in the braiding statistics and the  $S$ -matrix.

For  $k$  even,  $\det \tilde{S} = 1$  but for  $k$  odd  $\det \tilde{S} = 0$ . This singularity is explained by the isomorphism:

$$\tilde{S}_{j_1 j_2} \cong \begin{pmatrix} 1 & 1 \\ 1 & 1 \end{pmatrix} \otimes \tilde{S}_{\text{integer, integer}} \text{ for } k \text{ odd}. \quad (\text{A6})$$

Thus  $K_k$  is only a true TQFT for  $k$  even. Physically, the problem with odd  $k$  is that it is not possible to distinguish the isospin- $j$  particle from the isospin- $(k/2 - j)$  particle by any braiding operation<sup>32,36</sup>.

Planar arc diagrams lead both to  $K_k$ , via Fig. 7, and to  $SU(2)_k$ , via the Rumer-Teller-Weyl theorem on  $SU(2)$  representations (see Ref. 42 for an exposition of both). The subtle difference is that certain  $-1$ 's, Frobenius-Schur indicators, occur in the representation theory coming from the fact that the fundamental representation of  $SU(2)$  is *antisymmetrically* self-dual, whereas these signs are absent in Kauffman's theory.

We come now to  $\mathcal{DK}_k$ , the Drinfeld double of  $K_k$ . It is a subspace of functions on links in surface  $\times$  interval (same relations as listed for solid torus) and has its own naturally defined positive definite hermitian inner product and a unitary  $S$ -matrix,  $\tilde{S}$ <sup>41,43</sup>. When  $k$  is even

$$\mathcal{DK}_k \cong K_k^* \otimes_{\mathbb{C}} K_k \text{ as Hilbert spaces, and } \tilde{S} = \tilde{S} \otimes \tilde{S}, \quad (\text{A7})$$

when  $k$  is odd, we still have:

$$\mathcal{DK}_k \cong K_k^* \otimes_{\mathbb{C}} K_k, \\ \text{but now } \tilde{S} = T \otimes \tilde{S}_{\text{integer, integer}} \otimes \tilde{S}_{\text{integer, integer}}, \quad (\text{A8})$$

i.e.  $\tilde{S}$  is the tensor square of the nonsingular even part of  $\tilde{S}$  tensor  $T$ , the  $4 \times 4$   $S$  matrix of the level  $k = 1$  theory  $\mathcal{DK}_1$ . In Kitaev's "toric code" notation<sup>28</sup> the irreps of  $\mathcal{DK}_1$  are:  $\emptyset, e, m$ , and  $em$ ; the trivial, electric, magnetic, and electric and magnetic excitations respectively. The Lagrangian for this sector is that of  $\mathbb{Z}_2$  theory<sup>44</sup>.

In this basis:

$$T = \begin{matrix} & \emptyset & e & m & em \\ \emptyset & 1/2 & 1/2 & 1/2 & 1/2 \\ e & 1/2 & 1/2 & -1/2 & -1/2 \\ m & 1/2 & -1/2 & 1/2 & -1/2 \\ em & 1/2 & -1/2 & -1/2 & 1/2 \end{matrix} \quad (\text{A9})$$

The isomorphisms in Eqs. (A6)–(A8) can be made explicit as follows (see Refs. 32,36).

$K_k$  has basis  $0, \dots, k/2$ . Define  $\hat{i} = k - i$ ,  $0 \leq i \leq K$ . If  $k$  is odd then exactly one of  $i$  and  $\hat{i}$  is even; denote that one by  $i_e$ . So when  $k$  is odd we write  $i = (i_e, \sigma_i)$  where  $\sigma_i = +$  or  $-$  as  $i$  is even or odd so  $(i_e, +) = i_e$ ,  $(i_e, -) = \hat{i}_e$ .

$\mathcal{DK}_k^* \otimes \mathcal{DK}_k$  has basis  $(i, j, l, m)$ ,  $0 \leq i, j, l, m \leq k/2$ , and  $(i, j, l, m) = (i_e, \sigma_i, j_e, \sigma_j, l_e, \sigma_l, m_e, \sigma_m)$  in the case  $k = \text{odd}$ . Declare an isomorphism  $\theta$  from  $(\sigma_i, \sigma_j)$  and from  $(\sigma_l, \sigma_m)$  to the toric code excitations by:  $(+, +) \rightarrow \emptyset, (-, +) \rightarrow e, (+, -) \rightarrow m$ , and  $(-, -) \rightarrow em$ . Then to realize (A8), map  $(i, j, l, m)$  to  $(\theta(\sigma_i, \sigma_j), \theta(\sigma_l, \sigma_m), i_e, j_e, l_e, m_e)$ .

## APPENDIX B: NEARLY DEGENERATE PERTURBATION THEORY

Although for the purposes of this paper we do not use anything beyond the second-order perturbation theory, here we present a general scheme useful for extending this type of analysis to higher orders. In particular, three and four-dimer moves will appear as higher order terms in the effective Hamiltonian.

The perturbative scheme presented here closely follows that developed in Ref. 45. The idea is to recursively block-diagonalise the Hamiltonian, order by order eliminating terms that change the number of dimer collisions (a collision occurs when two dimers share a vertex). The resulting effective Hamiltonian then contains terms (up to a given order) that only connect states within sectors with a fixed number of such collisions. To proceed with this programme, we rewrite the original Hamiltonian (1) as

$$H = T_0 + T_1 + T_{-1} + T_X + T_{-X} + D + W. \quad (\text{B1})$$

Here  $T_0 + T_1 + T_{-1} + T_X + T_{-X} = -\sum_{(i,j)} t_{ij} (c_i^\dagger c_j + \text{h.c.})$ ,  $D = \sum_i \mu_i n_i + \sum_{(i,j) \in \infty, \notin \square} V_{ij} n_i n_j$  is the "low-energy" part of potential energy, while  $W$  combines the remaining "high-energy" terms in  $H$ , i.e. all dimer collision interactions.  $T_0, T_1$  and  $T_{-1}$  represent the dimer moves that respectively do not change, increase by one, or decrease by one the number of collisions.  $T_X$  results in a dimer ending on top of another dimer (double occupancy in the original particle language), while  $T_{-X}$  undoes that. Since we have already chosen  $U_0 = \infty$  thus restricting our attention to the single-occupancy subspace within which  $T_{\pm X}$  have zero matrix elements, we should drop these terms from our consideration. Notice that  $T_m^\dagger = T_{-m}$  and  $[T_m, W] = -mUT_m$ ,  $m = 0, \pm 1$ .

Our strategy is to recursively construct the operator  $iS$  such that a "rotated" Hamiltonian  $\tilde{H}$  given by

$$\tilde{H} = e^{iS} H e^{-iS} = H + [iS, H] + \frac{1}{2!} [iS, [iS, H]] + \dots \quad (\text{B2})$$

is block-diagonal as described above. As a first approximation, we choose  $iS^{(1)} = (T_1 - T_{-1})/U$  which leads to  $H^{(2)} = T_0 + D + W + ([T_1, D] - [T_{-1}, D] + [T_1, T_0] - [T_{-1}, T_0] - [T_{-1}, T_1])/U + O(x^3/U^2)$ , where  $x = \max\{t_{ij}, V_{ij}, \mu_i\}$  (here we follow the numbering convention of Ref. 45 where  $H^{(1)} \equiv H$ ). This procedure eliminates  $T_1$  and  $T_{-1}$  but generates a slew of smaller terms, all of which, except  $-[T_{-1}, T_1]/U$ , change the number of dimer collisions. The next step is to correct  $iS$  in order to eliminate these new unwanted terms, repeating this procedure recursively up to any given order. The number of terms rapidly gets out of hand, and we used Mathematica to keep track of them up to the fourth order (i.e. keeping terms of order  $x^4/U^3$ ).

We are particularly interested in the terms that connect states within the lowest energy, zero collisions sector. Thus we can write  $\tilde{H} = \tilde{H}' + \tilde{H}''$  where  $\tilde{H}''$  consists of terms vanishing in this sector (i.e. the matrix element  $\langle \alpha | \tilde{H}'' | \beta \rangle = 0$  for

any two proper dimer coverings  $|\alpha\rangle$  and  $|\beta\rangle$ ). Then the effective low-energy Hamiltonian is given to the fourth order by:

$$\begin{aligned}
\tilde{H}^{(4)} &= D - T_{-1}T_1/U \\
&- \left( \frac{1}{2}DT_{-1}T_1 + T_{-1}DT_1 - \frac{1}{2}T_{-1}T_1D + T_{-1}T_0T_1 \right) / U^2 \\
&+ \left( -\frac{1}{2}DDT_{-1}T_1 + DT_{-1}DT_1 - T_{-1}DDT_1 \right. \\
&\quad + T_{-1}DT_1D - \frac{1}{2}T_{-1}T_1DD + DT_{-1}T_0T_1 \\
&\quad \left. - T_{-1}DT_0T_1 - T_{-1}T_0DT_1 + T_{-1}T_0T_1D \right. \\
&\quad \left. - T_{-1}T_0T_0T_1 + T_{-1}T_1T_{-1}T_1 - \frac{1}{2}T_{-1}T_{-1}T_1T_1 \right) / U^3 \\
&= D - \frac{T_{-1}T_1}{U} + \frac{1}{2U^2} \{ T_{-1} [D, T_1] + \text{h.c.} \} + \frac{T_{-1}T_0T_1}{U^2} \\
&- \left( \frac{1}{2} \{ T_{-1} [D, [D, T_1]] + \text{h.c.} \} - \{ T_{-1}T_0 [D, T_1] + \text{h.c.} \} \right. \\
&\quad \left. - T_{-1}T_0T_0T_1 + T_{-1}T_1T_{-1}T_1 - \frac{1}{2}T_{-1}T_{-1}T_1T_1 \right) / U^3 \quad (\text{B3})
\end{aligned}$$

The advantage of rewriting this Hamiltonian using commutators such as  $[D, T_1]$  becomes clear if we recall that  $D = \sum_i \mu_i n_i + \sum_{(i,j) \in \mathfrak{D}, \neq \emptyset} V_{ij} n_i n_j$  is diagonal in the local position

basis. This allows us to combine the terms as follows:

$$\begin{aligned}
&\langle \alpha | \left( -T_{-1}T_1 + \frac{1}{2} (T_{-1} [D, T_1] + \text{h.c.}) \right. \\
&\quad \left. - \frac{1}{2} (T_{-1} [D, [D, T_1]] + \text{h.c.}) \right) | \beta \rangle \\
&= -\frac{1}{2} \left\{ \sum_n \left( 1 - \frac{d_n - d_\beta}{U} + \left( \frac{d_n - d_\beta}{U} \right)^2 \right) \right. \\
&\quad \left. \times \langle \alpha | T_{-1} | n \rangle \langle n | T_1 | \beta \rangle + (\alpha \leftrightarrow \beta) \right\} \quad (\text{B4})
\end{aligned}$$

and

$$\begin{aligned}
&\langle \alpha | (T_{-1}T_0T_1 - (T_{-1}T_0 [D, T_1] + \text{h.c.})) | \beta \rangle \\
&= \sum_n \left( \frac{1}{2} - \frac{d_n - d_\beta}{U} \right) \langle \alpha | T_{-1}T_0 | n \rangle \langle n | T_1 | \beta \rangle \\
&\quad + (\alpha \leftrightarrow \beta) \quad (\text{B5})
\end{aligned}$$

where  $|n\rangle$  is an excited state with one dimer collision and  $d_n, d_\beta$  are the eigenvalues of  $D$ . Written in form (B4),(B5), these terms explicitly depend only on local differences in the two dimer configurations rather than the expectation values of infinite sums  $D$ .

- 
- <sup>1</sup> D. C. Tsui, H. L. Stormer, and A. C. Gossard, Phys. Rev. Lett. **48**, 1559 (1982).
  - <sup>2</sup> S. Das Sarma and A. Pinczek, *Perspectives in quantum Hall effects : novel quantum liquids in low-dimensional semiconductor structures* (Wiley, New York, 1997).
  - <sup>3</sup> P. W. Anderson, Science **235**, 1196 (1987).
  - <sup>4</sup> S. A. Kivelson, D. S. Rokhsar, and J. P. Sethna, Phys. Rev. B **35**, 8865 (1987).
  - <sup>5</sup> V. Kalmeyer and R. B. Laughlin, Phys. Rev. Lett. **59**, 2095 (1987).
  - <sup>6</sup> R. B. Laughlin, Phys. Rev. Lett. **60**, 2677 (1988).
  - <sup>7</sup> R. B. Laughlin, Science **242**, 525 (1988).
  - <sup>8</sup> A. Fetter, C. Hanna, and R. Laughlin, Phys. Rev. B **39**, 9679 (1989).
  - <sup>9</sup> Y. Chen, F. Wilczek, E. Witten, and B. Halperin, Int. J. Mod. Phys. B p. 1001 (1989).
  - <sup>10</sup> N. Read and B. Chakraborty, Phys. Rev. B **40**, 7133 (1989).
  - <sup>11</sup> N. Read and S. Sachdev, Phys. Rev. Lett. **66**, 1773 (1991).
  - <sup>12</sup> N. Read and S. Sachdev, Int. J. Mod. Phys. B **5**, 219 (1991).
  - <sup>13</sup> X. G. Wen, Phys. Rev. B **44**, 2664 (1991).
  - <sup>14</sup> C. Mudry and E. Fradkin, Phys. Rev. B **49**, 5200 (1994), cond-mat/9309021.
  - <sup>15</sup> L. Balents, M. P. A. Fisher, and C. Nayak, Int. J. Mod. Phys. B **12**, 1033 (1998), cond-mat/9803086.
  - <sup>16</sup> T. Senthil and M. P. A. Fisher, Phys. Rev. B **62**, 7850 (2000), cond-mat/9910224.
  - <sup>17</sup> R. Moessner and S. L. Sondhi, Phys. Rev. Lett. **86**, 1881 (2001), cond-mat/0007378.
  - <sup>18</sup> L. Balents, M. P. A. Fisher, and S. M. Girvin, Phys. Rev. B **65**, 224412 (2002), cond-mat/0110005.
  - <sup>19</sup> T. Senthil and O. Motrunich, Phys. Rev. B **66**, 205104 (2002), cond-mat/0201320.
  - <sup>20</sup> O. I. Motrunich and T. Senthil, Phys. Rev. Lett. **89**, 277004 (2002), cond-mat/0205170.
  - <sup>21</sup> R. Willett, J. P. Eisenstein, H. L. Stormer, D. C. Tsui, A. C. Gossard, and J. H. English, Phys. Rev. Lett. **59**, 1776 (1987).
  - <sup>22</sup> W. Pan, J.-S. Xia, V. Shvarts, D. E. Adams, H. L. Stormer, D. C. Tsui, L. N. Pfeiffer, K. W. Baldwin, and K. W. West, Phys. Rev. Lett. **83**, 3530 (1999), cond-mat/9907356.
  - <sup>23</sup> G. Moore and N. Read, Nucl. Phys. B **360**, 362 (1991).
  - <sup>24</sup> M. Greiter, X. G. Wen, and F. Wilczek, Nucl. Phys. B **374**, 567 (1992).
  - <sup>25</sup> C. Nayak and F. Wilczek, Nucl. Phys. B **479**, 529 (1996), cond-mat/9605145.
  - <sup>26</sup> N. Read and E. Rezayi, Phys. Rev. B **654**, 16864 (1996), cond-mat/9609079.
  - <sup>27</sup> E. Fradkin, C. Nayak, A. Tsvetlik, and F. Wilczek, Nucl. Phys. B **516**, 704 (1998), cond-mat/9711087.
  - <sup>28</sup> A. Y. Kitaev, Ann. Phys. **303**, 2 (2003), quant-ph/9707021.
  - <sup>29</sup> M. H. Freedman, Found. Comput. Math. **1**, 183 (2001), quant-ph/0003128 and references therein.
  - <sup>30</sup> L. Kauffman and S. Lins, *Temperley Lieb Recoupling theory and invariants of 3-manifolds*. (Princeton Univ. Press, 1994), vol. 134 of *Ann. Math. Stud.*
  - <sup>31</sup> M. H. Freedman, Commun. Math. Phys. **234**, 129 (2003), quant-ph/0110060.
  - <sup>32</sup> M. Freedman, C. Nayak, K. Shtengel, K. Walker, and Z. Wang (2003), cond-mat/0307511.
  - <sup>33</sup> M. H. Freedman, M. J. Larsen, and Z. Wang, Commun. Math. Phys. **227**, 605 (2002), quant-ph/0001108.
  - <sup>34</sup> M. H. Freedman, M. J. Larsen, and Z. Wang, Commun. Math. Phys. **228**, 177 (2002).
  - <sup>35</sup> D. S. Rokhsar and S. A. Kivelson, Phys. Rev. Lett. **61**, 2376

- (1988).
- <sup>36</sup> M. Freedman, C. Nayak, K. Walker, and Z. Wang, unpublished.
- <sup>37</sup> B. Sutherland, *Phys. Rev. B* **37**, 3786 (1988).
- <sup>38</sup> D. Jetchev, private communication.
- <sup>39</sup> E. Witten, *Comm. Math. Phys.* **121**, 351 (1989).
- <sup>40</sup> V. G. Turaev, *Quantum Invariants of Knots and 3-Manifolds* (Walter de Gruyter, Berlin, New York, 1994).
- <sup>41</sup> C. Blanchet, N. Habegger, G. Masbaum, and P. Vogel, *Topology* **34**, 883 (1995).
- <sup>42</sup> G. Kuperberg, *Comm. Math. Phys.* **180**, 109 (1996).
- <sup>43</sup> B. Bakalov and A. Kirillov, *Lectures on Tensor Categories and Modular Functors*, vol. 21 of *University Lecture Series* (American Mathematical Society, 2001).
- <sup>44</sup> F. Wegner, *J. Math. Phys.* **2259**, 12 (1971).
- <sup>45</sup> A. H. MacDonald, S. M. Girvin, and D. Yoshioka, *Phys. Rev. B* **37**, 9753 (1988).
- <sup>46</sup> R. Moessner and S. L. Sondhi, unpublished.
- <sup>47</sup> C. Kenyon and E. Rémila, *Discrete Math.* **152**, 191 (1996).
- <sup>48</sup> This terminology, first used in Ref. 31, indicates the Drinfeld double of the Kauffman bracket version of the  $SU(2)$  topological quantum field theory (TQFT) at level  $k$ . The Kauffman bracket version neglects the  $-1$ 's derived from the Frobenius-Schur indicator.
- <sup>49</sup> Of course, small ring terms (or at least their kinetic parts) arise perturbatively – see Appendix B. E.g. a four-particle move described later in the paper as a “bow tie” move occurs at order 4.
- <sup>50</sup> The important feature of the triangular lattice, for us, will be that it is *not* bipartite. On the edges of a bipartite lattice, our models will have an additional, undesired, conserved quantity (integral winding numbers), so the triangular lattice gives the simplest realization.
- <sup>51</sup> A multiloop is a collection of non-intersecting loops and arcs on a surface. The end points of an arc are required to lie on the boundary of the surface, see Ref. 32.
- <sup>52</sup> See Ref. 29 where private communication with A. Kitaev and G. Kuperberg is referenced. The required family of commuting projectors is easily derived in the Turaev-Viro approach<sup>40</sup> by writing  $\text{surface} \times \text{interval}$ ,  $\Sigma \times I = \text{handle-body union 2-handles}$ . The disjoint attaching curves of the 2-handles yield the commuting projectors.
- <sup>53</sup> In this paper we use the term “frustration” in reference to a Hamiltonian which can be written as a sum of projectors yet has no zero-modes. In this sense, new terms breaking the extensive degeneracy down to a crystalline structure will introduce frustration.
- <sup>54</sup> If a lattice is bipartite, i.e.  $\mathcal{L} = \mathcal{L}_A \cup \mathcal{L}_B$  so that for any site  $a \in \mathcal{L}_A$  all of its neighbouring sites  $b \in \mathcal{L}_B$  and vice versa, then any dimer  $r \in \mathcal{R}$  can be oriented:  $r \equiv (a, b) = (a \leftarrow b)$  with the opposite rule for dimers  $j \in \mathcal{J}$ :  $j \equiv (a, b) = (a \rightarrow b)$ . Then the transition graph  $\mathcal{R} \cup \mathcal{J}$  consists of oriented loops (orientation of loops of length 2 is ambiguous but can be ignored – it is the essential loops that lead to conserved quantities). From the physical point of view, these oriented loops can be treated as “level sets” or “equipotentials” leading to the height representation with the conserved quantity being the overall tilt. Such conserved quantities severely restrict quantum dynamics and typically lead to either crystalline phases or gapless quantum critical points<sup>46</sup>.
- <sup>55</sup> D. Jetchev, private communication. For a rigorous proof of ergodicity in a similar setting see Ref. 47.
- <sup>56</sup> Recall that replacing the constant  $d$  with variables  $a$  and  $b$  adds an important degree of freedom to the model.